Cell-autonomous and redundant roles of Hey1 and HeyL in muscle stem cells: HeyL requires Hes1 to bind diverse DNA sites

Yu-taro Noguchi[1*], Miki Nakamura[1*], Nobumasa Hino[2], Jumpei Nogami[3], Sayaka Tsuji[2], Takahiko Sato[4], Lidan Zhang[1], Kazutake Tsujikawa[1], Toru Tanaka[2], Kohei Izawa[2], Yoshiaki Okada[2], Takefumi Doi[2], Hiroki Kokubo[5], Akihito Harada[3], Akiyoshi Uezumi[6], Manfred Gessler[7], Yasuyuki Ohkawa[3], So-ichiro Fukada[1]

[1]Laboratory of Molecular and Cellular Physiology, Graduate School of Pharmaceutical Sciences, Osaka University, 1-6 Yamadaoka, Suita, Osaka 565-0871, Japan

[2]Laboratory of Molecular Medicine, Graduate School of Pharmaceutical Sciences, Osaka University, 1-6 Yamadaoka, Suita, Osaka 565-0871, Japan

[3]Division of Transcriptomics, Medical Institute of Bioregulation, Kyushu University, Fukuoka 812-8582, Japan

[4]Department of Ophthalmology, Kyoto Prefectural University of Medicine, Kyoto 602-8566, Japan

[5]Department of Cardiovascular Physiology and Medicine, Graduate School of Biomedical and Health Sciences, Hiroshima University, 1-2-3 Kasumi, Minamiku, Hiroshima 734-8551, Japan

[6]Department of Geriatric Medicine, Tokyo Metropolitan Institute of Gerontology, Itabashi-ku, Tokyo 173-0015, Japan.

[7]Developmental Biochemistry, Theodor-Boveri-Institute / Biocenter, and Comprehensive Cancer Center Mainfranken, University of Wuerzburg, 97074 Wuerzburg, Germany

* These authors contributed equally

Abstract

The undifferentiated state of muscle stem (satellite) cells (MuSCs) is maintained by the canonical Notch pathway. Although three bHLH transcriptional factors, Hey1, HeyL, and Hes1, are considered to be potential effectors of the Notch pathway exerting anti-myogenic effects, neither HeyL nor Hes1 inhibits myogenic differentiation of myogenic cell lines. Furthermore, whether these factors work redundantly or cooperatively is unknown. Here, we showed cell-autonomous functions of Hey1 and HeyL in MuSCs using conditional and genetic null mice. Analysis of cultured MuSCs revealed anti-myogenic activity of both HeyL and Hes1. We found that HeyL forms heterodimeric complexes with Hes1 in living cells. Moreover, our ChIP-Seq experiments demonstrated that, compared with HeyL alone, HeyL-Hes1 heterodimer bound with high affinity to specific sites in the chromatin including the cis-element of Hey1. Finally, the analyses of myogenin promoter activity showed that HeyL and Hes1 acted synergistically to suppress myogenic differentiation. Collectively, those results suggest that HeyL and Hey1 function redundantly in MuSCs, and that HeyL requires Hes1 for effective DNA binding and biological activity.

Introduction

A muscle satellite cell (MuSC) is a physiologically adult stem cell having the abilities to self-renew and produce abundant daughter cells called myoblasts (Collins et al., 2005; Lepper et al., 2011; Sacco et al., 2008; Sambasivan et al., 2011). In a steady state, MuSCs remain quiescent and undifferentiated. The loss of MuSC-pool results in the defect of myogenic regeneration, therefore, the maintenance mechanism of MuSCs is critical for the homeostasis of skeletal muscle (Lepper et al., 2011; Sambasivan et al., 2011). Recent studies have revealed some of the molecules regulating the quiescent and undifferentiated state of adult MuSCs (Cheung and Rando, 2013; Fukada et al., 2013; Yamaguchi et al., 2015). Among them, canonical Notch signaling has emerged, as it is a major molecular mechanism that underlies the maintenance of adult MuSCs.

The Notch signaling pathway is an evolutionarily conserved intercellular signaling system and is required for cell fate decisions and patterning events (Lai, 2004). The Notch receptor family consists of four members (Notch1–4). When a Notch receptor is activated by binding to a ligand (Delta-like and Jagged), the cleaved Notch receptor (the intracellular domain of the Notch receptor) translocates to the nucleus

where it activates transcription of target genes through interaction with Rbp-J (also known as Cbf1) (Lai, 2004). This Rbp-J-mediated pathway represents the canonical Notch pathway. A pioneering study of Notch-mediated cell fata decision in mammalian cells was done using myogenic cell line, C2C12 (Lindsell et al., 1995). Subsequent studies showed that canonical Notch signaling exhibits anti-myogenic functions in myogenic cell line (Kato et al., 1997; Kuroda et al., 1999). However, the effector molecules exerting anti-myogenic function is still controversial (Buas et al., 2009).

As aforementioned, canonical Notch pathway is essential to keep the MuSCs in a quiescent and undifferentiated state; in the absence of Rbp-J, MuSC numbers decline quickly, and the myogenic differentiation factors MyoD and myogenin are upregulated (Bjornson et al., 2012; Mourikis et al., 2012). Double conditional mutagenesis in Notch1 and Notch2 shows similar phenotypes with Rbp-J-depleted MuSCs, indicating canonical Notch1/2-Rbp-J axis is the critical pathway for the adult MuSCs maintenance (Fujimaki et al., 2018). However, as similar to the myogenic cell line, the downstream molecules for maintaining adult MuSCs remains to be elucidated.

The best-known primary targets of canonical Notch signaling are the *Hes* (Hairy and enhancer of split) and *Hey* (Hes-related, also known as Hesr/Herp/Hrt/Gridlock/Chf) families of the bHLH transcriptional repressor genes, raising the question whether these factors mediate Notch signals to suppress myogenic differentiation. However, previous analyses using a myogenic cell line, C2C12 cells, had indicated HeyL or Hes1 did not suppress the differentiation (Buas et al., 2009; Shawber et al., 1996). Furthermore, HeyL did not bind to the cis-element of Hey1(Iso et al., 2003; Nakagawa et al., 2000), raising the question whether Hey1 and HeyL work redundantly. We reported previously that Hey1 and HeyL double knock-out mice (dKO), but neither Hey1 nor HeyL single KO mice, were impaired in generating quiescent MuSCs as a consequence of an increase in MyoD and myogenin expressions (Fukada et al., 2011). This resembles the phenotypes of Rbp-J conditional KO (cKO) and Notch1/2 double cKO mice (Bjornson et al., 2012; Fujimaki et al., 2018; Mourikis et al., 2012). In this study, genetically *Hey1*/*HeyL*-null mice were analyzed. HeyL is specifically expressed in MuSCs, but Hey1 is also expressed in endothelial cells (Fukada et al., 2011) of the skeletal muscle, giving rise to a possibility of non-cell-autonomous roles of Hey1 in the muscle. We therefore used here a conditional mutagenesis to demonstrate that Hey1/HeyL are required in a cell autonomous manner and maintenance of MuSCs,

and that in the absence Hey1/HeyL the cells upregulate MyoD and myogenin. Moreover, we investigate the mechanisms of Hey1/HeyL function redundantly and demonstrate that these factors form heterodimers with Hes1, and that, in particular, HeyL requires Hes1 to bind with a higher affinity to chromatin and repress myogenesis more efficiently. Our results explain the controversial findings that Notch signaling, but neither HeyL nor Hes1 can suppresses differentiation alone, and thus indicate that HeyL cooperates with Hes1.

Results

Hey1/HeyL are essential for maintaining muscle satellite cell pool in adult skeletal muscle

In order to ensure the cell autonomous and redundant roles of Hey1/L in MuSCs, it was necessary to use MuSC-specific conditional KO mice. In skeletal muscle, HeyL mRNA is exclusively expressed in MuSCs, similar to Myf5 and Pax7. But Hey1 mRNA is detected also in CD31-positive endothelial cells (Figure supplement 1A) (Fukada et al., 2011). Additionally, single HeyL KO mice do not show significant phenotypes including skeletal muscle and heart (Fischer et al., 2007; Fukada et al., 2011). Therefore, we conditionally depleted Hey1 genes in MuSCs using $Pax7^{CreERT2/+}$ mice (Lepper et al., 2009).

Hey1/L double-knockout mice (hereafter referred as dKO) mice used in previous studies showed decreased body weight and size. The MuSC number was already reduced by 7 days after birth (Fukada et al., 2011). In contrast to dKO mice, MuSC-specific conditional Hey1/L double knockout mice treated with tamoxifen (Tm) (hereafter referred as co-dKO; $Pax7^{CreERT2/+}::Hey1^{flox/-\ or\ flox/flox}::HeyL^{-/-}$ mice with Tm) did not exhibit apparent impairments. The body and muscle weight of co-dKO mice were comparable to those of littermate controls (Figure 1A). However, MuSC numbers were significantly reduced in co-dKO mice compared to control mice three weeks after Tm injection (Figure 1B). The cell size of co-dKO MuSCs was larger than that of control MuSCs (Figure 1B and 1C).

Next, we examined the time-dependency of the effect of Tm injection on the MuSCs. Unexpectedly, when we used mice older than 8 weeks, conditional Hey1/L double mutant mice untreated with Tm (hereafter referred as co-dMt; *Pax7*$^{CreERT2/+}$*::Hey1*$^{flox/-\ or\ flox/flox}$*::HeyL*$^{-/-}$ mice without Tm) mice showed a reduction in the number of MuSCs and in *Hey1* transcripts (Figure 1D-Figure supplement 1A). However, four-week-old co-dMt mice showed normal MuSCs numbers and *Hey1* transcript levels (Figure 1D-figure supplement 1B), indicating that MuSCs-pool in co-dMt mice was not affected during postnatal development like dKO mice, but MuSC-pool is not sustained in the absence of both Hey1 and HeyL.

The loss of MuSCs results in the impaired muscle regeneration. As shown in Figure 1E-H, both reduced weight of regenerated muscle and increased area of fibrosis were observed in co-dKO mice. Because our previous analyses of dKO MuSCs indicated that the absence of both Hey1 and HeyL had no impact on the MuSC-proliferation and myotube formation (Fukada et al., 2011), the impaired regeneration in co-dKO can result from the loss of the MuSC-pool in co-dKO mice. Taken together, an unexpected reduction of Hey1 in the Tm-untreated mice occurred after co-dMt mice were four weeks old. However, our studies demonstrate that Hey1 and HeyL are essential for maintaining the MuSC-pool via cell-autonomous roles, in addition to their roles in generating adult MuSCs, because the MuSC pool is established about three weeks after birth (White et al., 2010).

Impaired quiescent and undifferentiated state in conditional Hey1/HeyL KO MuSCs

To examine the effect of the absence of Hey and HeyL on undifferentiated state of MuSCs, the expression of myogenic differentiation markers, MyoD and myogenin, were investigated. As shown in Figure 2A and 2B, the increased number of MyoD+ or myogenin+ cells was detected in skeletal muscle sections of co-dKO mice. Consistent with Figure 1D, the decreased number of MuSCs on isolated single myofibers was observed in > four-week-old co-dMt mice. In addition, the analyses of isolated single myofibers also indicated increased MyoD+ or myogenin+ cells in co-dMt mice (9-week-old, Figure 2C and D).

Next, we examined the mRNA expression of *MyoD* and *myogenin* together with two other myogenic genes, *Myf5* and *Pax7*. Significantly increased expression of the *myogenin* gene was observed in both dKO and co-dKO/co-dMt MuSCs, but not in control and each single KO mice (Figure 2E and 2F), suggesting the redundant roles of Hey1 and HeyL in MuSCs. mRNA expression levels of *Myf5* genes was decreased or tendency to decrease in dKO and co-dKO/co-dMt MuSC. Hey1/L are considered to be transcriptional repressors (Heisig et al., 2012); therefore, these results suggested that the accelerated myogenic differentiation secondarily affected *Myf5* expression in co-dKO/co-dMt mice (Machado et al., 2017). Decreased expression of *Pax7* was observed in co-dMt MuSCs, but not in dKO and co-dKO MuSCs. One possibility is that one allele of *Pax7* was not transcribed in co-dMt compared to the control mice (*Hey1* $^{floxflox\ or\ flox/+}$*::HeyL*$^{-/-}$ mice). Therefore, the genetic construct might have affected the decreased *Pax7* expression in co-dMt. The *MyoD* mRNA expression level was not changed in either dKO or co-dKO/co-dMt compared to control or single KO mice.

Anti-myogenic effects of Hey1, HeyL, and Hes1 in primary myoblasts

Our data demonstrate that Hey1 and HeyL function redundantly to maintain the undifferentiated state of MuSCs *in vivo*. However, HeyL did not exhibit remarkable anti-myogenic effects in a myogenic cell line (C2C12), as observed with Hey1 (Figure supplement 2)(Buas et al., 2009). Hes1, another critical target of Notch signaling also does not have an anti-myogenic effect in C2C12 (Figure supplement 2) (Shawber et al., 1996). In order to examine the impact of Hey1, HeyL, and Hes1 on primary myoblasts, each gene was retrovirally expressed in primary myoblasts, and MyoD expression was quantified. As shown in Figure 3A and 3B, both the percentage of MyoD-positive cells and *MyoD* mRNA expression were significantly reduced by Hey1-expression, indicating that Hey1 had a significant anti-myogenic effect on primary myoblasts, as observed in C2C12. On the other hand, HeyL did not alter the percentage of MyoD-positive cells, but increased the number of MyoD-low cells and suppressed *MyoD* mRNA expression (Figure 3A and 3B). Furthermore, HeyL slightly, but significantly, reduced myotube formation (Figure 3C), indicating that HeyL has anti-myogenic effects on primary myoblasts. Hes1 remarkably suppressed the MyoD level in primary myoblasts (Figure 3D). Taken together, although HeyL and Hes1 were considered to have no anti-myogenic effect based on the study of C2C12 cells, these

results indicate that both HeyL and Hes1 exerted the anti-myogenic effect in a more physiological type of cells, primary myoblasts as observed in other group (Wen et al., 2012).

HeyL and Hes1 form heterodimers in living cells

The different effects of HeyL and Hes1 on primary myoblasts and the C2C12 cell line implied three possibilities: 1) the absence of a co-repressor for Hes1 or HeyL, 2) the absence of each heterodimer partner, or 3) both in C2C12. Thus, we examined the necessity of Hes1 for HeyL because Hes1 and HeyL have the possibility to work as a heterodimer (Jalali et al., 2011). First, we assayed the existence of HeyL-Hes1 heterodimers in living cells using a site-specific photo-crosslink technique (Hino et al., 2005; Kita et al., 2016), (Figure 4A). For successful photo-cross-linking between interacting proteins, a photo-cross-linkable amino acid, N□-(meta-trifluoromethyl-diazirinyl-benzyloxycarbonyl)-l-lysine (mTmdZLys) should be incorporated near the binding interface of the proteins. We decided to introduce mTmdZLys into the Orange and bHLH domains of HeyL at the positions indicated in Figure 4B and 4C because Hey and Hes1 form homodimers via these domains (Iso et al., 2001), and formation of heterodimers of the proteins via the same domains was expected. Each mTmdZLys-containing and C-terminal FLAG-tagged HeyL mutant was expressed in 293 c18 cells, together with C-terminal myc-tagged Hes1 protein. After exposure of the cells to UV light, HeyL complexes were purified from extracts of the cells with an anti-FLAG antibody, and then analyzed by Western blotting with an anti-myc antibody. As shown in Figure 4D, a product with a molecular mass of ~70 kDa, which almost corresponds to the sum of the masses of HeyL (35 kDa) and Hes1 (30 kDa), was detected depending on the exposure to UV light. This result indicates a photo-cross-linking of HeyL with Hes1, i.e., a heterodimer formation of the proteins in living cells. A similar result was obtained for Hey1, indicating heterodimerization with Hes1 (Figure 4B, 4C and 4E). Hey1 and HeyL also formed a heterodimer complex (Figure supplement 3A). On the other hand, neither Hey1 nor HeyL formed heterodimers with MyoD (Figure 4F and 4G), and Hes1 formed a heterodimer with MyoD much less efficiently than with HeyL (Figure 4F and 4G, and Figure supplement 3B and 3C). Taken together, HeyL and Hes1 can form a heterodimer, perhaps to exert their effective functions.

HeyL-Hes1 heterodimer complex binds to more diverse DNA sites than HeyL alone

In order to elucidate the functional difference between HeyL alone and the HeyL-Hes1 heterodimer, chromatin-immunoprecipitated (ChIP) assays were performed using doxycycline-dependent HeyL alone or C2C12 cells expressing HeyL-Hes1 (Figure 5A). HeyL- or Hes1-expressing cells were sorted by EGFP (enhanced green fluorescent protein) or mKO (monomeric Kusabira orange) fluorescence, respectively (Figure 5B). A FLAG-tag was fused to *HeyL* genes, but not *Hes1 genes*; therefore, we used an anti-FLAG antibody for immunoprecipitation assays, followed by sequencing (ChIP-seq). Genome-wide binding profiles showed that there was a notable difference between HeyL alone and HeyL-Hes1 cistromes (Figure 5C). The number of ChIP-seq peaks for HeyL-Hes1 was constantly greater than that for HeyL alone at various *P*-value thresholds (Figure 5D), suggesting that HeyL-Hes1 has more binding sites than HeyL alone. Figure 5E shows the signals for a HeyL-Hes1 heterodimer and HeyL alone along with the histone modifications H3K27ac, H3K27me3, and H3K4me3. HeyL-Hes1 binding sites overlapped with H3K27ac and H3K4me3, which indicates that HeyL-Hes1 preferentially bound to active proximal promoter regions. Importantly, the list of enriched motifs around HeyL-Hes1 peaks included the cis-element of Hey1, CACGTG, and a Hes1-binding site, CACGCG (Figure 5F). In the case of HeyL alone, we did not detect enriched motifs with a significant difference. Compared with HeyL alone, higher signal levels of HeyL-Hes1 in Hey1 and Hes1 promoter regions are consistent with the fact that Hey1 and Hes1 negatively regulate their own mRNA expression (Figure 5G). Chip-PCR analyses of the Hes1 promoter containing the Hey1-binding site (CACGTG) indicated that HeyL-Hes1 bound to the cis-element of Hey1 more efficiently than HeyL alone, as well as with Hey1 alone or Hey1-Hes1 (Figure 5H). Chip-PCR analyses of the Hey1 promoter containing the Hes1-binding site (CACGCG, Hey1 also binds to this motif (Heisig et al., 2012)) also showed similar results (Figure 5H). These results suggest that HeyL can bind the Hey1-cis element in concert with Hes1, which also supports the redundant roles of Hey1 and HeyL in MuSCs.

Finally, we examined the synergistic effects of Hes1 and HeyL using myogenin-promoter activity instead of MyoD for the following reasons: 1) MyoD mRNA levels were not different between dKO and co-dKO. 2) The myogenin promoter includes a Hey1 binding site (Buas et al., 2010). 3) Suppression mechanisms of myogenin might be more critical for MuSCs than that of MyoD because myogenin

expression induced irreversible terminal differentiation. 4) Recent studies showed MyoD mRNA is abundant in quiescent MuSCs (de Morree et al., 2017). As in the previous report, Hey1 suppressed myogenin promoter activity in a dose-dependent manner. In contrast, neither HeyL nor Hes1 had an effect (Figure supplement 4). However, the co-existence of HeyL and Hes1 remarkably suppressed myogenin-luciferase activity, indicating that HeyL requires Hes1 to exert the anti-myogenic effect (Figure 5I).

Discussion

Canonical Notch signaling is a critical pathway to maintain the undifferentiated state of MuSCs (Bjornson et al., 2012; Fujimaki et al., 2018; Mizuno et al., 2015; Mourikis et al., 2012). However, the downstream effectors exerting the anti-myogenic effects have not been identified. Neither HeyL nor Hes1 have inhibitory effects on myogenic differentiation and myogenic gene expression in a C2C12 cell line (Buas et al., 2009; Shawber et al., 1996), whereas Hey1 has (Buas et al., 2009)(data shown here). Sasai et al showed that Hes1 inhibited MyoD-induced myogenic conversion of fibroblasts (Sasai et al., 1992). The reported data suggested that Hes1 deprived E47 from MyoD/E47 heterodimer complexes, which inhibited MyoD-induced myogenic conversion. In our and Shawbers' analyses, Hes1 did not inhibit the MyoD-dependent myogenin-promoter activity. The discrepancy between Sasai's and our results could be explained by the dependency of E47 in each analysis. In fact, Sasai et al. showed that Hes1 did not inhibit the function of MyoD homodimers and did not bind to the E-box strongly. Importantly, our results proposed that, in contrast to Hes1 alone, the Hes1-HeyL heterodimer binds the E-box strongly.

Notch signaling still exerted an anti-myogenic effect in Hey1 suppressed C2C12 cells by the siRNA (Buas et al., 2009), indicating that inhibition of myogenesis by Notch consists of redundant or multiple pathways. Our current study implies that HeyL-Hes1 and Hey1 homodimer/heterodimer are two essential units downstream of the canonical Notch pathway in MuSCs (Figure 6). This model does not explain the full picture of anti-myogenic mechanisms in the Notch pathway. When Hey1, HeyL, and Hes1 was silenced in C2C12 cells, the Notch ligand still inhibited MyoD and myogenin mRNA expression (data not shown), suggesting there are other effectors for the anti-myogenic roles of Notch besides Hey1, HeyL, and Hes1. This speculation is

supported by the results of Pax3-Cre::Rbp-J and our Hey1/L dKO mice. The depletion of Rbp-j by Pax3-Cre produced a severe muscle developmental defect compared with Hey1/L dKO mice (Fukada et al., 2011; Vasyutina et al., 2007), indicating that the anti-myogenic effects of canonical Notch signaling during embryogenesis depend on something other than Hey1 and HeyL. Thus, additional members of the Hes/Hey family might also participate in the suppression of embryonic myogenesis, or other mechanisms that do not rely on Hes/Hey factors might be active. However, MuSCs require Hey1 and HeyL for entry into quiescence and for their maintenance.

Those members of the Hes and Hey family form heterodimeric complexes has been described before (Fischer and Gessler, 2007; Iso et al., 2001; Jalali et al., 2011). However, to our knowledge, there is no evidence showing a physiological role of Hes-Hey heterodimer complexes. Our present study is the first that indicates the physiological importance of the HeyL-Hes1 heterodimer for maintaining MuSCs in the undifferentiated state. A remaining question is why HeyL prefers to form a heterodimer with Hes1 rather than forming HeyL homodimers or Hey1-HeyL heterodimers. In addition, we did not succeed to suppress myogenic differentiation by co-expression of HeyL-Hes1 in C2C12 cells similar to the results when HeyL or Hes1 were expressed separately (data not shown). *Myogenin*-luciferase analyses do not depend on the existence of a co-repressor when HeyL-Hes1 occupies MyoD binding sites. ChIP-seq analyses are also independent of the existence of a co-repressor, suggesting that C2C12 cells do not express a functional co-repressor for Hey1 or Hes1. On the contrary, the existence of functional co-repressor for Hes1 in the primary myoblast explains the significant anti-myogenic effect of Hes1. The identification of the co-repressor(s) that interact with Hes/Hey factors will lead to a better understanding of the mechanisms that maintains the undifferentiated state of MuSCs.

In this study, we analyzed the myogenin promoter as a target gene of Hes/Hey. In considering an undifferentiated state of MuSCs, the regulatory mechanism of MyoD (upstream of myogenin) expression attracts attention. In Rbp-J coKO, Hey1/L-double null and Hey1/L co-dKO mice, the frequency of MyoD+ MuSC was dramatically increased, but mRNA expression of *MyoD* was not changed or decreased in those three KO MuSCs (Bjornson et al., 2012; Fukada et al., 2011; Mourikis et al., 2012). This might indicate that the translation of *MyoD* mRNA is accelerated in MuSCs by losing canonical Notch signaling. Zismanov et al. reported that phosphorylation of serine51 of

eIF2a is necessary to maintain MuSCs in an undifferentiated and quiescent state (Zismanov et al., 2016). MuSCs unable to phosphorylate eIF2alpha exited quiescence and activated the myogenic program, which included an upregulation of the MyoD protein level. eIF2a is a key regulator of mRNA translational, which means *MyoD* mRNA is present even in quiescent MuSCs but the protein is not produced, similar to Myf5, another myogenic determination gene (Crist et al., 2012). Intriguingly, de Morree et al. reported that quiescent MuSCs include abundant *MyoD* mRNA and an RNA binding protein, Staufen, that suppresses the translation of *MyoD* mRNA (de Morree et al., 2017). On the other hand, Machado et al. showed that the *MyoD* transcription level in quiescent MuSCs is much weaker than that in activated MuSCs, and the *MyoD* transcription level is up-regulated during MuSC isolation (Machado et al., 2017). The necessity of transcriptional regulation of MyoD in quiescent MuSCs is controversial, but Hey1, HeyL, and Hes1 are candidate factors for suppressing *MyoD* transcription because they can suppress the *MyoD* transcriptional level in primary myoblasts. Sun et al. reported that Hey1 suppressed MyoD-dependent activation of the myogenin promoter by forming MyoD-Hey1 complexes (Sun et al., 2001). On the other hand, Buas et al. argued against formation of a MyoD-Hey1 complex (Buas et al., 2010). Using photo-cross linking analyses, we detected neither MyoD-Hey1 nor MyoD-HeyL complexes. Notably, MuSCs do not express MyoD on the protein level; therefore, these results suggest that the anti-myogenic effect of both Hey1 and HeyL in MuSCs are independent of the formation of a heterodimer with MyoD.

We expected that genetic inactivation of *Hey1* would be induced in $Pax7^{CreERT2/+}$::$Hey1^{flox/- \text{ or } flox/flox}$ mice by Tm injection. $Pax7^{CreERT2/+}$ mice have been widely used, and we have also reported tamoxifen-dependent depletion of *Calcr* genes (Yamaguchi et al., 2015). One reason of the unexpected result is the effect of *Pax7* haploinsufficiency because *Pax7* is transcribed from one allele in the $Pax7^{CreERT2/+}$ mice. However, we also had similar results using tomato-RFP mice and the $Pax7^{CreERT2/+}$ mice (Figure supplement 5), suggesting the leaky activation of Cre recombinase. The mechanism evoking leaky activation of Cre recombinase is unknown because CreERT2 is a modified enzyme providing higher specificity compared to CreER (Indra et al., 1999). However, we observed significant differences in MuSC number between $Pax7^{CreERT2/+}$::$Hey1^{flox/+}$::$HeyL^{-/-}$ and $Pax7^{CreERT2/+}$::$Hey1^{flox/- \text{ or } flox/flox}$::$HeyL^{-/-}$mice

with/without Tm, indicating that Hey1 and HeyL are necessary for maintaining MuSCs as well as generating MuSCs during the postnatal development.

In conclusion, our results indicate Hey1 and HeyL maintain the undifferentiated state of MuSCs in a cell autonomous and redundant manner as effectors of canonical Notch signaling. We also demonstrated here that HeyL requires Hes1 for an efficient DNA binding including the Hey1 cis-element. The undifferentiated state of MuSCs could be defined by non-expression of MyoD, but the transcriptional expression of MyoD in quiescent MuSCs is controversial. Further analyses of MyoD transcriptional regulation and the target genes and co-repressor of HeyL-Hes1 will lead to elucidation of the maintenance mechanisms of MuSCs.

Materials and Methods

Mice

Hey1-/- allele and HeyL-/- mice were generated as described before (Fukada et al., 2011; Kokubo et al., 2005). Hey1-floxed mice were generated by Fischer et al. (Fischer et al., 2005). *Pax7*$^{CreERT2/+}$ (Lepper et al., 2009) mice were obtained from Jackson Laboratories. All procedures for experimental animals were approved by the Experimental Animal Care and Use Committee at Osaka University.

Muscle injury

Muscles were injured by injecting cardiotoxin (2.5 μL per g of mouse body weight of 10 μM in saline, Sigma-Aldrich, St. Louis, MO) into the tibialis anterior (TA) muscle.

Preparation and FACS analyses of skeletal muscle-derived mononuclear cells

Mononuclear cells from uninjured limb muscles were prepared using 0.2% collagenase type II (Worthington Biochemical Corp., Lakewood, NJ) as previously described (Uezumi et al., 2006).

Mononuclear cells derived from skeletal muscle were stained with FITC-conjugated anti-CD31, CD45, phycoerythrin-conjugated anti-Sca-1, and biotinylated-SM/C-2.6 (Fukada et al., 2004) antibodies. Cells were then incubated with streptavidin-labeled allophycocyanin (BD Biosciences, San Diego, CA) on ice for 30

min, and resuspended in PBS containing 2% FCS and 2 μg/ml PI. Cell sorting was performed using an FACS Aria II™ flow cytometer (BD Immunocytometry Systems, Mountain View, CA). Debris and dead cells were excluded by forward scatter, side scatter, and PI gating. Data were collected using FACSDiva™ software (BD Biosciences).

Single myofiber culture and staining

Single myofibers were isolated from extensor digitorum longus muscles following the previously described protocol (Rosenblatt et al., 1995). Fixation and immunostaining followed described protocols (Shinin et al., 2009). Anti-Pax7, -MyoD, and -myogenin antibodies were purchased from Developmental Studies Hybridoma Bank (Iowa City, IA, USA), Santa Cruz Biotechnology (Dallas, TX, USA), and DAKO (Clone: F5D, Glostrup, Denmark), respectively. The images were obtained using a BZ-X700fluorescence microscope (Keyence Osaka, Japan).

RT-PCR

Total RNA was extracted from sorted or cultured cells with a Qiagen RNeasy Mini Kit according to the manufacturer's instructions (Qiagen, Hilden, Germany) and then reverse-transcribed into cDNA by using TaqMan Reverse Transcription Reagents (Roche Diagnostics, Mannheim, Germany). A polymerase chain reaction (PCR) was performed with cDNA and specific primers. Primer pairs were published in previous reports (Yamaguchi et al., 2015).

Histology

Tibialis anterior muscles were isolated and frozen in liquid nitrogen-cooled isopentane (Wako Pure Chemical Industries). Transverse cryosections (10 μm) were stained with hematoxylin and eosin (H&E).

Immunohistochemistry

For immunohistological analyses, transverse cryosections (7 μm) were fixed with 4% PFA for 10 min. Anti-Pax7, -MyoD, and -myogenin antibodies were the same as those used in the single myofiber staining. Anti-collagen type I and anti-laminin α2 antibody were purchased from Bio-Rad (Hercules, CA, USA) and Enzo Life Sciences (clone

4H8-2, Enzo Life Sciences, Inc. Plymouth Meeting, PA, USA), respectively. The anti-M-cadherin antibody was described in a previous study (Yamaguchi et al., 2015). For mouse anti-Pax7, a MOM kit (Vector Laboratories, Burlingame, CA, USA) was used to block endogenous mouse IgG before reaction with the primary antibodies. The signals were recorded photographically using a BZ-X700 fluorescence microscope, and collagen type I-positive areas were quantified by Hybrid Cell Count software (Keyence).

Retroviral vector preparation and infection experiments

The viral particles (retro pCLIG-Hey1, pCLIG-HeyL, parental retro pCLIG, pMX-Hes1, parental retro pMX) were prepared as described (Morita et al., 2000). MuSCs were isolated from C57BL/6 mice, and were plated on dishes coated with Matrigel in GM. After 3 d, GFP-positive cells were collected by cell sorting. After an additional 2 d culture in GM, the cells were fixed and stained with anti-MyoD antibody (Clone 5.8A, BD Biosciences). To examine the effects of Hey1 and HeyL on differentiation of MuSCs, GFP-positive cells were cultured in DM for an additional 3 d, and then stained with anti-sarcomeric α-actinin antibody (Clone: EA-53, Sigma-Aldrich).

Photo-cross-linking in living cells

Site-specific incorporation of mTmdZLys into HeyL protein in living cells with an expanded genetic code was performed as described previously (Kita et al., 2016). In brief, a pOriP plasmid containing a HeyL gene with an amber non-sense (TAG) mutation in the positions shown in Figure 4D was transfected into 293 c18 cells, together with the plasmids containing the gene variants for an amber suppressor pyrrolysine tRNA and a mTmdZLys-specific pyrrolysyl-tRNA synthetase. The cells were incubated in DMEM supplemented with mTmdZLys at a final concentration with 10 μM for 16 h, the amino acid was incorporated at the amber position, resulting in the expression of HeyL protein as a full-length form. To analyze heterodimer formation, a pcDNA4/TO plasmid containing the Hes1 gene was co-transfected with the abovementioned plasmids. For protein photo-cross-linking, the cells were exposed to UV light (λ = 365 nm) for 15 min. Extraction, purification, and Western blot analysis of cross-linked products were performed as described previously (Kita et al., 2016). The

analyses of the heterodimerization of proteins other than Hey1-Hes1were performed in a similar way.

Doxycline-inducible Hey and Hes1 construct and cell line selection

Stably expressed clones were obtained through transfections of pT2A-TRETIBI/EGFP-Hey1, EGFP-HeyL and mKO-Hes1 using Lipofectamine 2000 (Life Technologies, Carlsbad, CA, USA). C2C12 cells at 20–30% confluence were transfected with an expression vector (4 μg plasmid DNA per 100-mm plate), pCAGGS-TP coding transposase (provided by Dr. Kawakami) and pT2A-CAG-rtTA2S-M2 and incubated for 24 h. EGFP- or mKO-positive cells were sorted by an FACS AriaII to select stably expressed clones.

ChIP-seq assay (NGS) and data analysis

ChIP libraries of HeyL alone and HeyL-Hes1 were prepared with the NEBNext Ultra DNA Library Prep Kit for Illumina (New England Biolabs, Ipswich, MA). They were sequenced on an Illumina HiSeq 1500. The reads were then aligned to the mouse reference genome (GRCm38) with the software HISAT2 version 2.0.4 (Kim et al., 2015)). Only uniquely mapped reads were considered for subsequent analysis. The aggregation map was prepared using *plotProfile* of the deepTools suite version 2.5.1 (Ramirez et al., 2016). Peaks were identified using the caller BCP version 1.1 (Xing et al., 2012) at various p-value cut-offs (p-values $<10^{-6}$, 10^{-7}, and 10^{-8}, the last of which is the default value). The heat map was drawn with deepTools' *plotHeatmap,* where H3K4me3 and H3K27me3 data are from ENCODE (ENCSR000AHO and ENCSR000AHR respectively) and H3K27ac data from Rudnicki Laboratory (GSE37525). Motif enrichment analysis was performed using CentriMo (Bailey and Machanick, 2012); the search was filtered so that it yields results from the database JASPAR CORE 2016 vertebrates. The target coverage was calculated using the number of region matches. Our data accession number is DRA006432 (DDBJ).

ChIP-PCR analysis

C2C12 cells were crosslinked with 1% formaldehyde, and sonicated for 15 cycles at 15 s/cycle using a Sonifer Model 250 (Branson, Danbury, CT, U.S.A.) with an output control of 2 and a duty cycle of 30%. The extract was incubated at 4°C for 24 h with

Dynabeads (Invitrogen, #10003D) pre-coated with 3 µg antibodies against FLAG (Sigma-Aldrich, #F1804) and control IgG (Cell Signaling, #5415). The DNA‐protein complexes were collected using a magnet, and de-crosslinked in a solution containing 50 mM Tris‐HCl (pH 8.0), 10 mM EDTA, and 1% sodium dodecyl sulfate. The resulting DNA was analyzed by real-time PCR with specific primers.

Luciferase assay

All vectors were transfected in C2C12 by X-tremeGENE 9 DNA Transfection Reagent (Roche). The 3.8kb fragment of myogenin regulatory element was amplified by PCR (Fujisawa-Sehara et al., 1993). The fragment was ligated into a pGL4.23 vector cut with XhoI and Bgl2, and the sequence was examined. A pRL *Renilla* Luciferase Reporter Vector was used for normalizing the transfection efficiency. Forty hours after transfection, the cells were harvested and lysed using Dual-Luciferase Reporter Assay System (Promega), and then luciferase activity was measured on a GLOMAX-MULTI detection system (Promega). Data indicate the expression relative to the basal level of *Myogenin*-luciferase co-transfected with empty expression vectors.

Statistics

Values were expressed as means ± SD. Statistical significance was assessed by Student's *t* test. In comparisons of more than two groups, non-repeated measures analysis of variance (ANOVA) followed by the Bonferroni test (vs control) or SNK test (multiple comparisons) were used. A probability of less than 5% ($p<0.05$) or 1% ($p<0.01$) was considered statistically significant.

Acknowledgement

We sincerely thank Prof. Toshio Kitamura for providing the pMXs vector and packaging cells. We also thank Prof. Ryoichiro Kageyama for pCLIG-Hey1, -HeyL vectors, Dr. Kensaku Sakamoto and Dr. Shigeyuki Yokoyama for pOriP vectors, and Prof. Seiji Takashima for providing mTmdZLys. This work was supported by a Grant-in Aid for Young Scientists (A) (S.F.), Grant-in-Aid for Scientific Research (B) (S.F.), an Intramural Research Grant for Neurological and Psychiatric Disorders of NCNP (S.F.), and the Suzuken Memorial Foundation (S.F.). This research was also supported by AMED under Grant Number 18am0101084j0002 (K.T.).

We thank Katherine Ono for comments on the manuscript.

References

Bailey, T.L., and Machanick, P. (2012). Inferring direct DNA binding from ChIP-seq. *Nucleic Acids Res* **40**, e128.

Bjornson, C.R., Cheung, T.H., Liu, L., Tripathi, P.V., Steeper, K.M., and Rando, T.A. (2012). Notch signaling is necessary to maintain quiescence in adult muscle stem cells. *Stem Cells* **30**, 232-242.

Buas, M.F., Kabak, S., and Kadesch, T. (2009). Inhibition of myogenesis by Notch: evidence for multiple pathways. *J Cell Physiol* **218**, 84-93.

Buas, M.F., Kabak, S., and Kadesch, T. (2010). The Notch effector Hey1 associates with myogenic target genes to repress myogenesis. *J Biol Chem* **285**, 1249-1258.

Cheung, T.H., and Rando, T.A. (2013). Molecular regulation of stem cell quiescence. *Nature reviews. Molecular cell biology* **14**, 329-340.

Collins, C.A., Olsen, I., Zammit, P.S., Heslop, L., Petrie, A., Partridge, T.A., and Morgan, J.E. (2005). Stem cell function, self-renewal, and behavioral heterogeneity of cells from the adult muscle satellite cell niche. *Cell* **122**, 289-301.

Crist, C.G., Montarras, D., and Buckingham, M. (2012). Muscle satellite cells are primed for myogenesis but maintain quiescence with sequestration of Myf5 mRNA targeted by microRNA-31 in mRNP granules. *Cell Stem Cell* **11**, 118-126.

de Morree, A., van Velthoven, C.T.J., Gan, Q., Salvi, J.S., Klein, J.D.D., Akimenko, I., Quarta, M., Biressi, S., and Rando, T.A. (2017). Staufen1 inhibits MyoD translation to actively maintain muscle stem cell quiescence. *Proc Natl Acad Sci U S A* **114**, E8996-E9005.

Fischer, A., and Gessler, M. (2007). Delta-Notch--and then? Protein interactions and proposed modes of repression by Hes and Hey bHLH factors. *Nucleic Acids Res* **35**, 4583-4596.

Fischer, A., Klattig, J., Kneitz, B., Diez, H., Maier, M., Holtmann, B., Englert, C., and Gessler, M. (2005). Hey basic helix-loop-helix transcription factors are repressors of GATA4 and GATA6 and restrict expression of the GATA target gene ANF in fetal hearts. *Mol Cell Biol* **25**, 8960-8970.

Fischer, A., Steidl, C., Wagner, T.U., Lang, E., Jakob, P.M., Friedl, P.,

Knobeloch, K.P., and Gessler, M. (2007). Combined loss of Hey1 and HeyL causes congenital heart defects because of impaired epithelial to mesenchymal transition. *Circ Res* **100**, 856-863.

Fujimaki, S., Seko, D., Kitajima, Y., Yoshioka, K., Tsuchiya, Y., Masuda, S., and Ono, Y. (2018). Notch1 and Notch2 Coordinately Regulate Stem Cell Function in the Quiescent and Activated States of Muscle Satellite Cells. *Stem Cells* **36**, 278-285.

Fujisawa-Sehara, A., Hanaoka, K., Hayasaka, M., Hiromasa-Yagami, T., and Nabeshima, Y. (1993). Upstream region of the myogenin gene confers transcriptional activation in muscle cell lineages during mouse embryogenesis. *Biochem Biophys Res Commun* **191**, 351-356.

Fukada, S., Higuchi, S., Segawa, M., Koda, K., Yamamoto, Y., Tsujikawa, K., Kohama, Y., Uezumi, A., Imamura, M., Miyagoe-Suzuki, Y., *et al.* (2004). Purification and cell-surface marker characterization of quiescent satellite cells from murine skeletal muscle by a novel monoclonal antibody. *Exp Cell Res* **296**, 245-255.

Fukada, S., Ma, Y., Ohtani, T., Watanabe, Y., Murakami, S., and Yamaguchi, M. (2013). Isolation, characterization, and molecular regulation of muscle stem cells. *Frontiers in physiology* **4**, 317.

Fukada, S., Yamaguchi, M., Kokubo, H., Ogawa, R., Uezumi, A., Yoneda, T., Matev, M.M., Motohashi, N., Ito, T., Zolkiewska, A., *et al.* (2011). Hesr1 and Hesr3 are essential to generate undifferentiated quiescent satellite cells and to maintain satellite cell numbers. *Development* **138**, 4609-4619.

Heisig, J., Weber, D., Englberger, E., Winkler, A., Kneitz, S., Sung, W.K., Wolf, E., Eilers, M., Wei, C.L., and Gessler, M. (2012). Target gene analysis by microarrays and chromatin immunoprecipitation identifies HEY proteins as highly redundant bHLH repressors. *PLoS Genet* **8**, e1002728.

Hino, N., Okazaki, Y., Kobayashi, T., Hayashi, A., Sakamoto, K., and Yokoyama, S. (2005). Protein photo-cross-linking in mammalian cells by site-specific incorporation of a photoreactive amino acid. *Nat Methods* **2**, 201-206.

Indra, A.K., Warot, X., Brocard, J., Bornert, J.M., Xiao, J.H., Chambon, P., and Metzger, D. (1999). Temporally-controlled site-specific mutagenesis in

the basal layer of the epidermis: comparison of the recombinase activity of the tamoxifen-inducible Cre-ER(T) and Cre-ER(T2) recombinases. *Nucleic Acids Res* **27**, 4324-4327.

Iso, T., Kedes, L., and Hamamori, Y. (2003). HES and HERP families: multiple effectors of the Notch signaling pathway. *J Cell Physiol* **194**, 237-255.

Iso, T., Sartorelli, V., Poizat, C., Iezzi, S., Wu, H.Y., Chung, G., Kedes, L., and Hamamori, Y. (2001). HERP, a novel heterodimer partner of HES/E(spl) in Notch signaling. *Mol Cell Biol* **21**, 6080-6089.

Jalali, A., Bassuk, A.G., Kan, L., Israsena, N., Mukhopadhyay, A., McGuire, T., and Kessler, J.A. (2011). HeyL promotes neuronal differentiation of neural progenitor cells. *J Neurosci Res* **89**, 299-309.

Kato, H., Taniguchi, Y., Kurooka, H., Minoguchi, S., Sakai, T., Nomura-Okazaki, S., Tamura, K., and Honjo, T. (1997). Involvement of RBP-J in biological functions of mouse Notch1 and its derivatives. *Development* **124**, 4133-4141.

Kim, D., Langmead, B., and Salzberg, S.L. (2015). HISAT: a fast spliced aligner with low memory requirements. *Nat Methods* **12**, 357-360.

Kita, A., Hino, N., Higashi, S., Hirota, K., Narumi, R., Adachi, J., Takafuji, K., Ishimoto, K., Okada, Y., Sakamoto, K., *et al.* (2016). Adenovirus vector-based incorporation of a photo-cross-linkable amino acid into proteins in human primary cells and cancerous cell lines. *Scientific reports* **6**, 36946.

Kokubo, H., Miyagawa-Tomita, S., Nakazawa, M., Saga, Y., and Johnson, R.L. (2005). Mouse hesr1 and hesr2 genes are redundantly required to mediate Notch signaling in the developing cardiovascular system. *Dev Biol* **278**, 301-309.

Kuroda, K., Tani, S., Tamura, K., Minoguchi, S., Kurooka, H., and Honjo, T. (1999). Delta-induced Notch signaling mediated by RBP-J inhibits MyoD expression and myogenesis. *J Biol Chem* **274**, 7238-7244.

Lai, E.C. (2004). Notch signaling: control of cell communication and cell fate. *Development* **131**, 965-973.

Lepper, C., Conway, S.J., and Fan, C.M. (2009). Adult satellite cells and embryonic muscle progenitors have distinct genetic requirements. *Nature*

460, 627-631.

Lepper, C., Partridge, T.A., and Fan, C.M. (2011). An absolute requirement for Pax7-positive satellite cells in acute injury-induced skeletal muscle regeneration. *Development* **138**, 3639-3646.

Lindsell, C.E., Shawber, C.J., Boulter, J., and Weinmaster, G. (1995). Jagged: a mammalian ligand that activates Notch1. *Cell* **80**, 909-917.

Machado, L., Esteves de Lima, J., Fabre, O., Proux, C., Legendre, R., Szegedi, A., Varet, H., Ingerslev, L.R., Barres, R., Relaix, F.*, et al.* (2017). In Situ Fixation Redefines Quiescence and Early Activation of Skeletal Muscle Stem Cells. *Cell reports* **21**, 1982-1993.

Mizuno, S., Yoda, M., Shimoda, M., Tohmonda, T., Okada, Y., Toyama, Y., Takeda, S., Nakamura, M., Matsumoto, M., and Horiuchi, K. (2015). A Disintegrin and Metalloprotease 10 (ADAM10) Is Indispensable for Maintenance of the Muscle Satellite Cell Pool. *J Biol Chem* **290**, 28456-28464.

Morita, S., Kojima, T., and Kitamura, T. (2000). Plat-E: an efficient and stable system for transient packaging of retroviruses. *Gene therapy* **7**, 1063-1066.

Mourikis, P., Sambasivan, R., Castel, D., Rocheteau, P., Bizzarro, V., and Tajbakhsh, S. (2012). A critical requirement for Notch signaling in maintenance of the quiescent skeletal muscle stem cell state. *Stem Cells* **30**, 243-252.

Nakagawa, O., McFadden, D.G., Nakagawa, M., Yanagisawa, H., Hu, T., Srivastava, D., and Olson, E.N. (2000). Members of the HRT family of basic helix-loop-helix proteins act as transcriptional repressors downstream of Notch signaling. *Proc Natl Acad Sci U S A* **97**, 13655-13660.

Ramirez, F., Ryan, D.P., Gruning, B., Bhardwaj, V., Kilpert, F., Richter, A.S., Heyne, S., Dundar, F., and Manke, T. (2016). deepTools2: a next generation web server for deep-sequencing data analysis. *Nucleic Acids Res* **44**, W160-165.

Rosenblatt, J.D., Lunt, A.I., Parry, D.J., and Partridge, T.A. (1995). Culturing satellite cells from living single muscle fiber explants. *In Vitro Cell Dev Biol Anim* **31**, 773-779.

Sacco, A., Doyonnas, R., Kraft, P., Vitorovic, S., and Blau, H.M. (2008). Self-renewal and expansion of single transplanted muscle stem cells. *Nature* **456**, 502-506.

Sambasivan, R., Yao, R., Kissenpfennig, A., Van Wittenberghe, L., Paldi, A., Gayraud-Morel, B., Guenou, H., Malissen, B., Tajbakhsh, S., and Galy, A. (2011). Pax7-expressing satellite cells are indispensable for adult skeletal muscle regeneration. *Development* **138**, 3647-3656.

Sasai, Y., Kageyama, R., Tagawa, Y., Shigemoto, R., and Nakanishi, S. (1992). Two mammalian helix-loop-helix factors structurally related to Drosophila hairy and Enhancer of split. *Genes Dev* **6**, 2620-2634.

Shawber, C., Nofziger, D., Hsieh, J.J., Lindsell, C., Bogler, O., Hayward, D., and Weinmaster, G. (1996). Notch signaling inhibits muscle cell differentiation through a CBF1-independent pathway. *Development* **122**, 3765-3773.

Shinin, V., Gayraud-Morel, B., and Tajbakhsh, S. (2009). Template DNA-Strand Co-Segregation and Asymmetric Cell Division in Skeletal Muscle Stem Cells, Vol 482 (Humana Press).

Sun, J., Kamei, C.N., Layne, M.D., Jain, M.K., Liao, J.K., Lee, M.E., and Chin, M.T. (2001). Regulation of myogenic terminal differentiation by the hairy-related transcription factor CHF2. *J Biol Chem* **276**, 18591-18596.

Uezumi, A., Ojima, K., Fukada, S., Ikemoto, M., Masuda, S., Miyagoe-Suzuki, Y., and Takeda, S. (2006). Functional heterogeneity of side population cells in skeletal muscle. *Biochem Biophys Res Commun* **341**, 864-873.

Vasyutina, E., Lenhard, D.C., Wende, H., Erdmann, B., Epstein, J.A., and Birchmeier, C. (2007). RBP-J (Rbpsuh) is essential to maintain muscle progenitor cells and to generate satellite cells. *Proc Natl Acad Sci U S A* **104**, 4443-4448.

Wen, Y., Bi, P., Liu, W., Asakura, A., Keller, C., and Kuang, S. (2012). Constitutive Notch activation upregulates Pax7 and promotes the self-renewal of skeletal muscle satellite cells. *Mol Cell Biol* **32**, 2300-2311.

White, R.B., Bierinx, A.S., Gnocchi, V.F., and Zammit, P.S. (2010). Dynamics of muscle fibre growth during postnatal mouse development. *BMC Dev Biol* **10**, 21.

Xing, H., Mo, Y., Liao, W., and Zhang, M.Q. (2012). Genome-wide localization of protein-DNA binding and histone modification by a Bayesian change-point method with ChIP-seq data. *PLoS Comput Biol* **8**, e1002613.

Yamaguchi, M., Watanabe, Y., Ohtani, T., Uezumi, A., Mikami, N., Nakamura, M., Sato, T., Ikawa, M., Hoshino, M., Tsuchida, K.*, et al.* (2015). Calcitonin Receptor Signaling Inhibits Muscle Stem Cells from Escaping the Quiescent State and the Niche. *Cell reports* **13**, 302-314.

Zismanov, V., Chichkov, V., Colangelo, V., Jamet, S., Wang, S., Syme, A., Koromilas, A.E., and Crist, C. (2016). Phosphorylation of eIF2alpha Is a Translational Control Mechanism Regulating Muscle Stem Cell Quiescence and Self-Renewal. *Cell Stem Cell* **18**, 79-90.

Figures

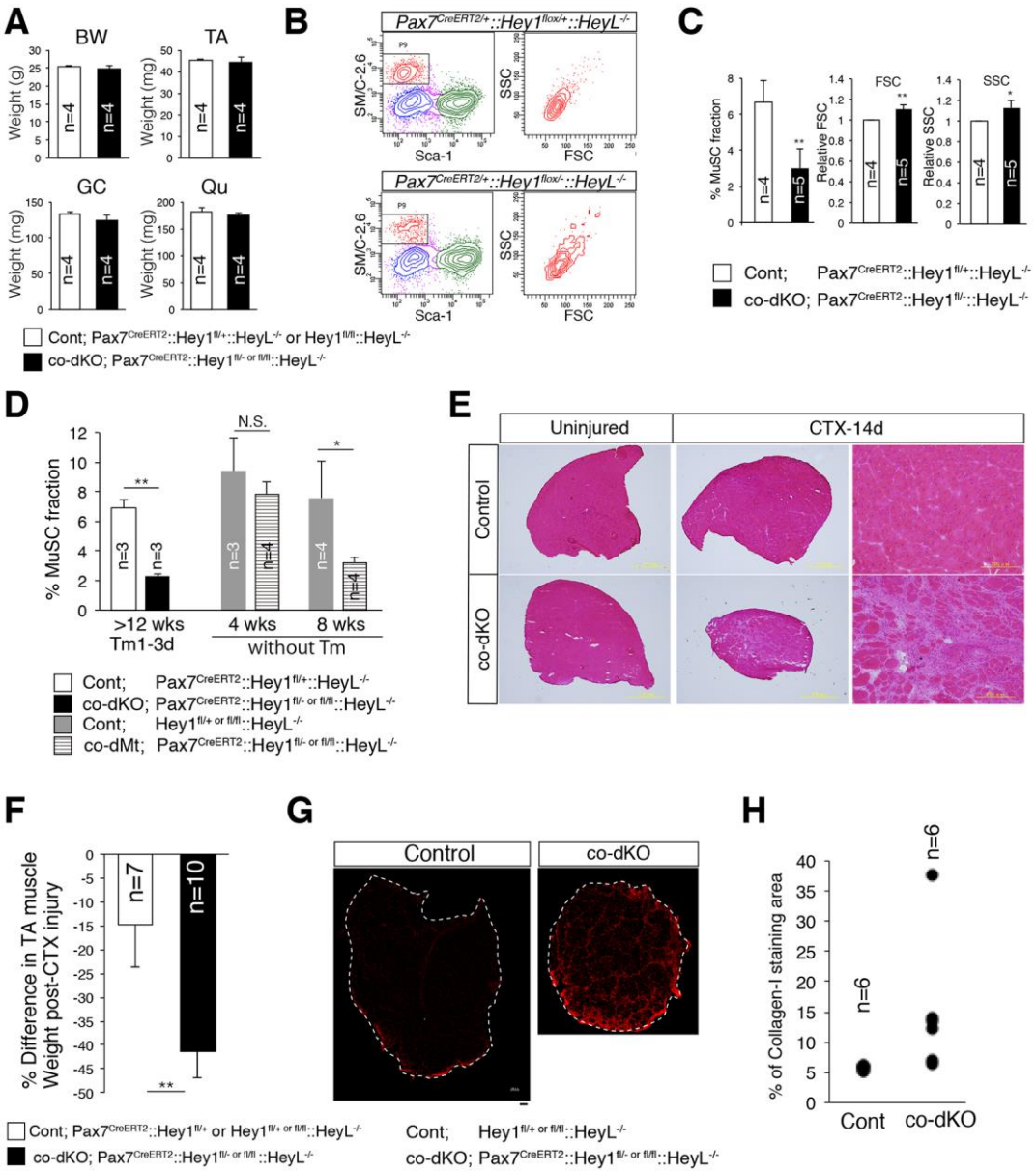

Figure 1: Muscle stem cell numbers and regenerative ability are reduced in conditional Hey1/HeyL double knockout mice.

(A) Body weight (B.W., g), tibialis anterior (TA), gastrocnemius (GC), and quadriceps (Qu) muscle weights (mg) of control (White bar; *Pax7$^{CreERT2/+}$::Hey1$^{flox/+}$::HeyL$^{-/-}$ or Hey1^{floxflox}::HeyL$^{-/-}$*) or co-dKO (Black; *Pax7$^{CreERT2/+}$::Hey1$^{flox/-\ or\ flox/flox}$::HeyL$^{-/-}$*) male mice at 10 weeks old 2 weeks after tamoxifen (Tm) injection. The *Y*-axis shows the

mean with s.d. The numbers in the graph show the number of mice analyzed in this Figure.

(B) FACS profiles of mononuclear cells derived from control (*Pax7*$^{CreERT2/+}$*::Hey1*$^{flox/+}$*::HeyL*$^{-/-}$) or co-dKO (*Pax7*$^{CreERT2/+}$*::Hey1*$^{flox/-}$*::HeyL*$^{-/-}$) muscles. The left profiles were gated for CD31^{-} CD45^{-} fractions. The right profiles show the cell size (FSC) and cell granularity (SSC) of MuSC fractions (SM/C-2.6^{+}CD31^{-}CD45^{-}Sca1^{-}).

(C) The mean percentage, the relative FSC (forward scatter), or the relative SSC (side scatter) of MuSC derived from control (*Pax7*$^{CreERT2/+}$*::Hey1*$^{flox/+}$*::HeyL*$^{-/-}$) or co-dKO (*Pax7*$^{CreERT2/+}$*::Hey1*$^{flox/-}$*::HeyL*$^{-/-}$) muscles 7 to 19 days after Tm injection. *, P<0.05; **, P<0.01.

(D) Quantitative analyses of MuSC number by flow cytometer. The y-axis shows the percentage of SM/C-2.6^{+}CD31^{-}CD45^{-}Sca1^{-} cells in control (White bar; *Pax7*$^{CreERT2/+}$*::Hey1*$^{flox/+}$*::HeyL*$^{-/-}$; 1 to 3 days after Tm, Gray bar; *Hey1*$^{flox/flox\ or\ flox/+}$*::HeyL*$^{-/-}$; without injection Tm), co-dKO mice (Black bar; *Pax7*$^{CreERT2/+}$*::Hey1*$^{flox/-\ or\ flox/flox}$*::HeyL*$^{-/-}$; 1 to 3 days after Tm), or co-dMt (Stripe bar; *Pax7*$^{CreERT2/+}$*::Hey1*$^{flox/-\ or\ flox/flox}$*::HeyL*$^{-/-}$ without Tm) at the indicated age or date. The X-axis shows the mean with s.d. *; P<0.05; **, P<0.01.

(E) Histological analyses (H.E. staining) of control (*Hey1* $^{flox/+}$*:HeyL*$^{-/-}$) and co-dKO (*Pax7*$^{CreERT2/+}$*::Hey1*$^{flox/-}$*::HeyL*$^{-/-}$) muscles 2 weeks after cardiotoxin (CTX) injection.

(F) The change in TA muscle weight 2 weeks after CTX injection in control (White bar; *Pax7*$^{CreERT2/+}$*::Hey1*$^{flox/+}$*::HeyL*$^{-/-}$ *or Hey1*$^{floxflox\ or\ flox/+}$*::HeyL*$^{-/-}$; 5 weeks after Tm injection) or co-dKO (Black bar; *Pax7*$^{CreERT2/+}$*::Hey1*$^{flox/-\ or\ flox/flox}$*::HeyL*$^{-/-}$; 5 weeks after Tm injection) mice. 10 to 16-week-old mice were treated with Tm. **, P<0.01.

(G) Immunohistochemical staining for collagen type I (red) in control (*Hey1*$^{flox/+}$*::HeyL*$^{-/-}$; 5 weeks after Tm injection) or co-dKO (*Pax7*$^{CreERT2/+}$*::Hey1* $^{flox/flox}$*::HeyL*$^{-/-}$; 5 weeks after Tm injection) muscle 2 weeks after CTX injection. Scale bar: 100 μm.

(H) Quantitative analyses of collagen type I-positive area in control (*Hey1*$^{floxflox\ or\ flox/+}$*::HeyL*$^{-/-}$; 5 weeks after Tm) and co-dKO mice (*Pax7*$^{CreERT2/+}$*::Hey1*$^{flox/-\ or\ flox/flox}$*::HeyL*$^{-/-}$; 5 weeks after Tm injection) 2 weeks after CTX injection. 10 to 16-week-old mice were treated with Tm.

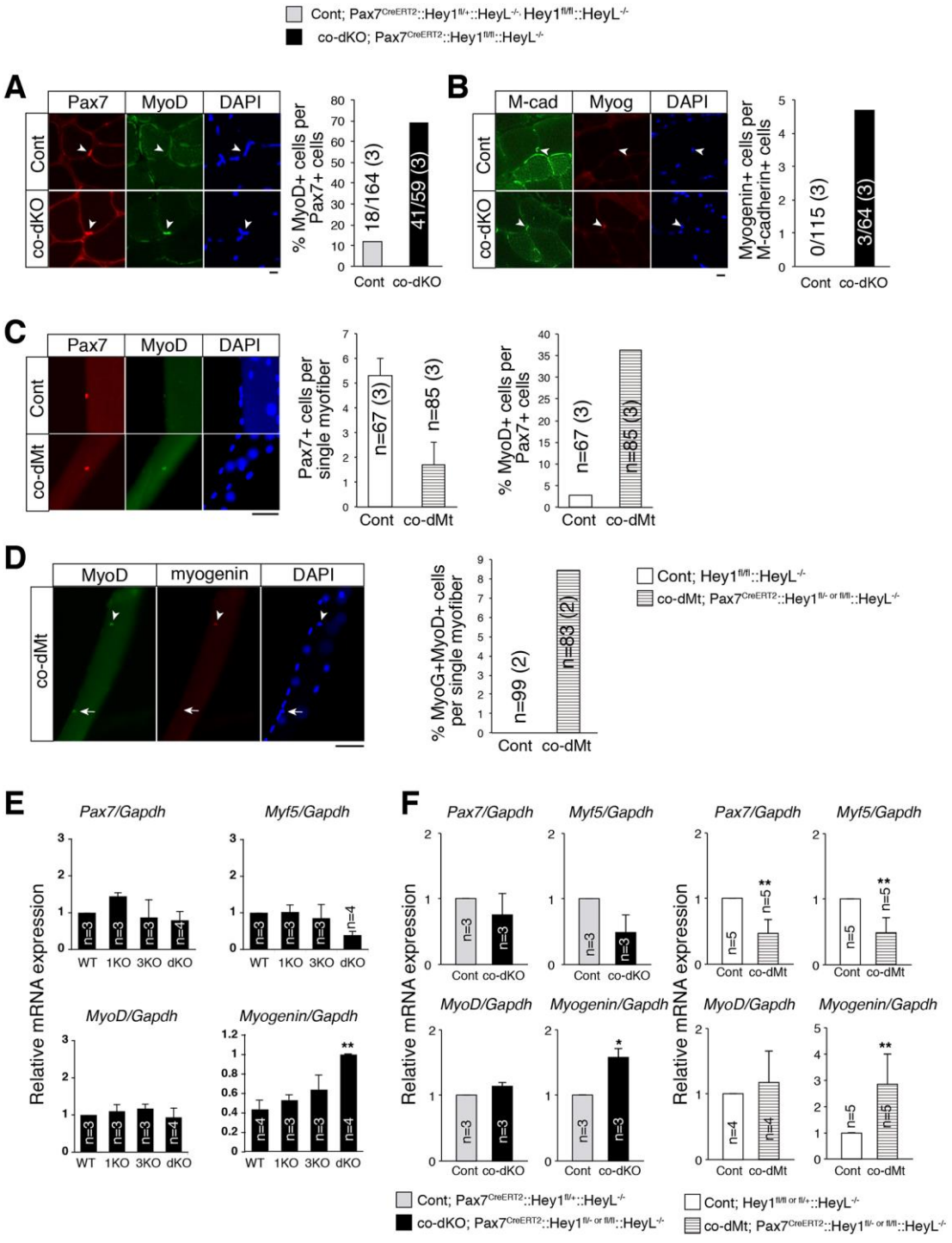

Figure 2: Undifferentiated state is impaired in Hey1/L-conditional KO mice.

(A) Uninjured TA muscles of control and co-dKO mice at 10 weeks old were stained with anti-Pax7 (red) and MyoD (green) antibodies. Arrowheads shows muscle stem cells. Scale bar: 10 μm. The right graphs indicate the frequency of MyoD+ cells per

Pax7+ cell in control (Gray bar; *Hey1*^{floxflox}*::HeyL*$^{-/-}$; 2 weeks after Tm injection) and co-dKO mice (Black bar; *Pax7*$^{CreERT2/+}$*::Hey1* $^{flox/flox}$*::HeyL*$^{-/-}$; 2 weeks after Tm injection). The number of marker-positive MuSCs among total counted MuSCs is indicated in each bar. The number in parentheses shows the number of mice used for analyses.

(B) Uninjured TA muscles of 10-week-old control and co-dKO mice were stained with anti-M-cadherin (M-cad; green) and myogenin (Myog; red) antibodies. Arrowheads shows muscle stem cells. Scale bar: 10 μm. The right graphs indicate the frequency of myogenin+ cell per M-cadherin+ cells in control (Gray bar; *Hey1*^{floxflox}*::HeyL*$^{-/-}$; 2 weeks after Tm injection) and co-dKO (Black bar; *Pax7*$^{CreERT2/+}$*::Hey1* $^{flox/flox}$*::HeyL*$^{-/-}$; 2 weeks after Tm injection) mice. The number of marker-positive MuSCs among total counted MuSCs is indicated in each bar. The number in parentheses shows the number of mice used for analyses.

(C) Freshly isolated single myofibers were stained with anti-Pax7 (red) and MyoD (green) antibodies. Scale bar: 50 μm. The right graphs indicate the number of Pax7+ cells per single myofiber or the percentage of MyoD+ cells in Pax7+ cells in control (White bar; *Hey1*^{floxflox}*::HeyL*$^{-/-}$) and co-dMt (Stripe bar; *Pax7*$^{CreERT2/+}$*::Hey1* $^{flox/flox}$*::HeyL*$^{-/-}$) mice. The number of myofibers counted is indicated in each bar. The number in parentheses shows the number of mice used for analyses. 9-week-old mice were used.

(D) Freshly isolated single myofibers were stained with anti-MyoD (green) and myogenin (red) antibodies. Arrowheads and arrows show MyoD+/myogenin+ and MyoD+/myogenin- cells, respectively. Scale bar: 50 μm. The right graph indicates the percentage of MyoD+myogenin+ cells per single myofiber in control (White bar; *Hey1*^{floxflox}*::HeyL*$^{-/-}$) and co-dMt (Stripe bar; *Pax7*$^{CreERT2/+}$*::Hey1* $^{flox/flox}$*::HeyL*$^{-/-}$) mice. The number of myofibers counted is indicated in each bar. The number in parentheses shows the number of mice used for analyses. 9-week-old mice were used.

(E) Relative mRNA expression of myogenic genes in freshly isolated MuSCs derived from WT, 1KO (Hey1-KO), 3KO (HeyL-KO), or dKO (Hey1/L-dKO) mice. 10 to 12-week-old mice were used. **, $P<0.01$.

(F) Relative mRNA expression of myogenic genes in freshly isolated MuSCs derived from Cont (Gray bar; *Pax7*$^{CreERT2/+}$*::Hey1* $^{flox/+}$*::HeyL*$^{-/-}$ 2 weeks after Tm,), co-dKO (Black bar; *Pax7*$^{CreERT2/+}$*::Hey1* $^{flox/flox\ or\ flox/-}$*::HeyL*$^{-/-}$ 2 weeks after Tm,), Cont (White

bar; *Hey1*$^{floxflox\ or\ flox/+}$*::HeyL*$^{-/-}$ without Tm), or co-dMt (Stripe bar; *Pax7*$^{CreERT2/+}$*::Hey1* $^{flox/flox\ or\ flox/-}$*::HeyL*$^{-/-}$ without Tm) mice. 8 to 14-week-old mice were analyzed in this study **; P<0.01.

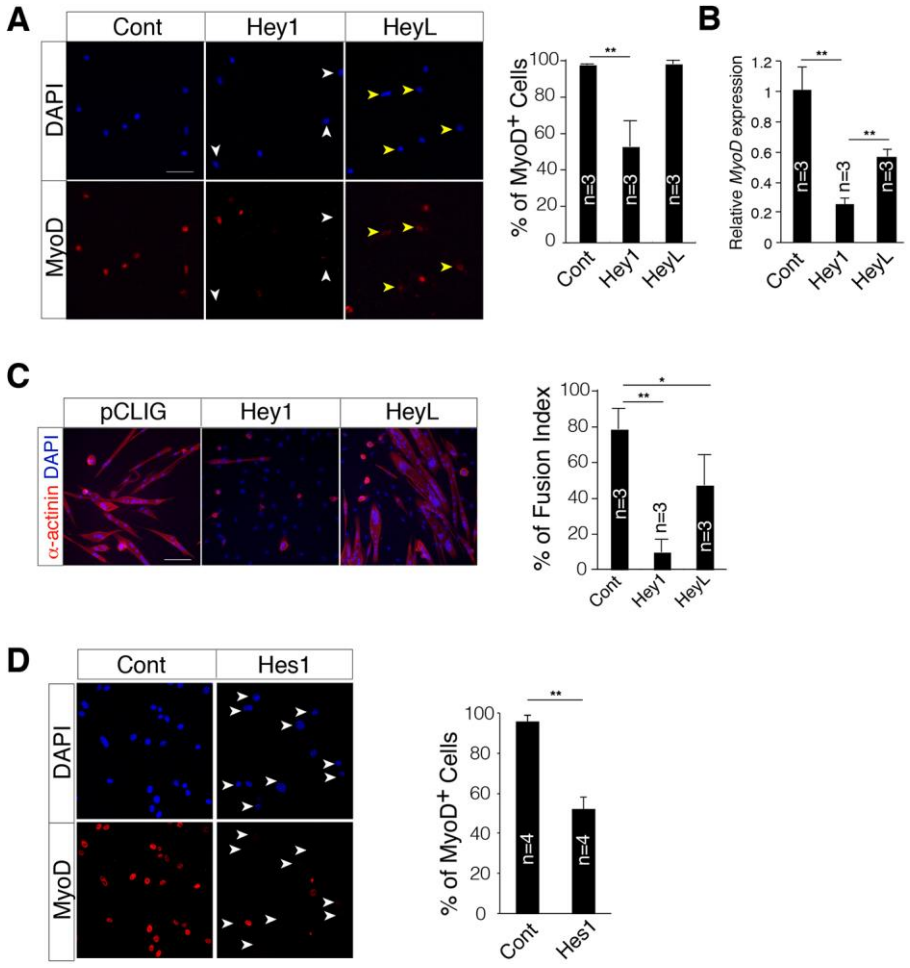

Figure 3: HeyL or Hes1 shows anti-myogenic effect in primary myoblasts

(A) Proliferating MuSCs were infected with each retrovirus construct: Cont: parental vector expressing GFP; Hey1: Hey1 and GFP-expressing vector; HeyL: HeyL and GFP-expressing vector. Sorted and cultured GFP+ cells were stained for MyoD. White or yellow arrowheads indicate MyoD- or MyoD^{low} cells, respectively. Scale bar: 100 μm. The right graph indicates the percentage of MyoD+ cells in Cont, Hey1-, or HeyL-expressing cells obtained from three independent experiments. **, P<0.01.

(B) Relative mRNA expression of MyoD in Cont, Hey1-, or HeyL-expressing cells obtained from three independent experiments.. **, P<0.01.

(C) Immunostaining for alpha-sarcomeric actinin (red). The right graph indicates fusion index of Cont, Hey1- or HeyL-expressing cells.

(D) Proliferating MuSCs were infected with each retrovirus construct: Cont: parental vector expressing GFP; Hes1: Hes1- and GFP-expressing vector. Sorted and cultured GFP+ cells were stained for MyoD. Arrows indicate MyoD- cells. Scale bar: 100 μm.

The right graph indicates the percentage of MyoD+ cells in Cont or Hes1-expressing cells obtained from four independent experiments.. **, $P<0.01$.

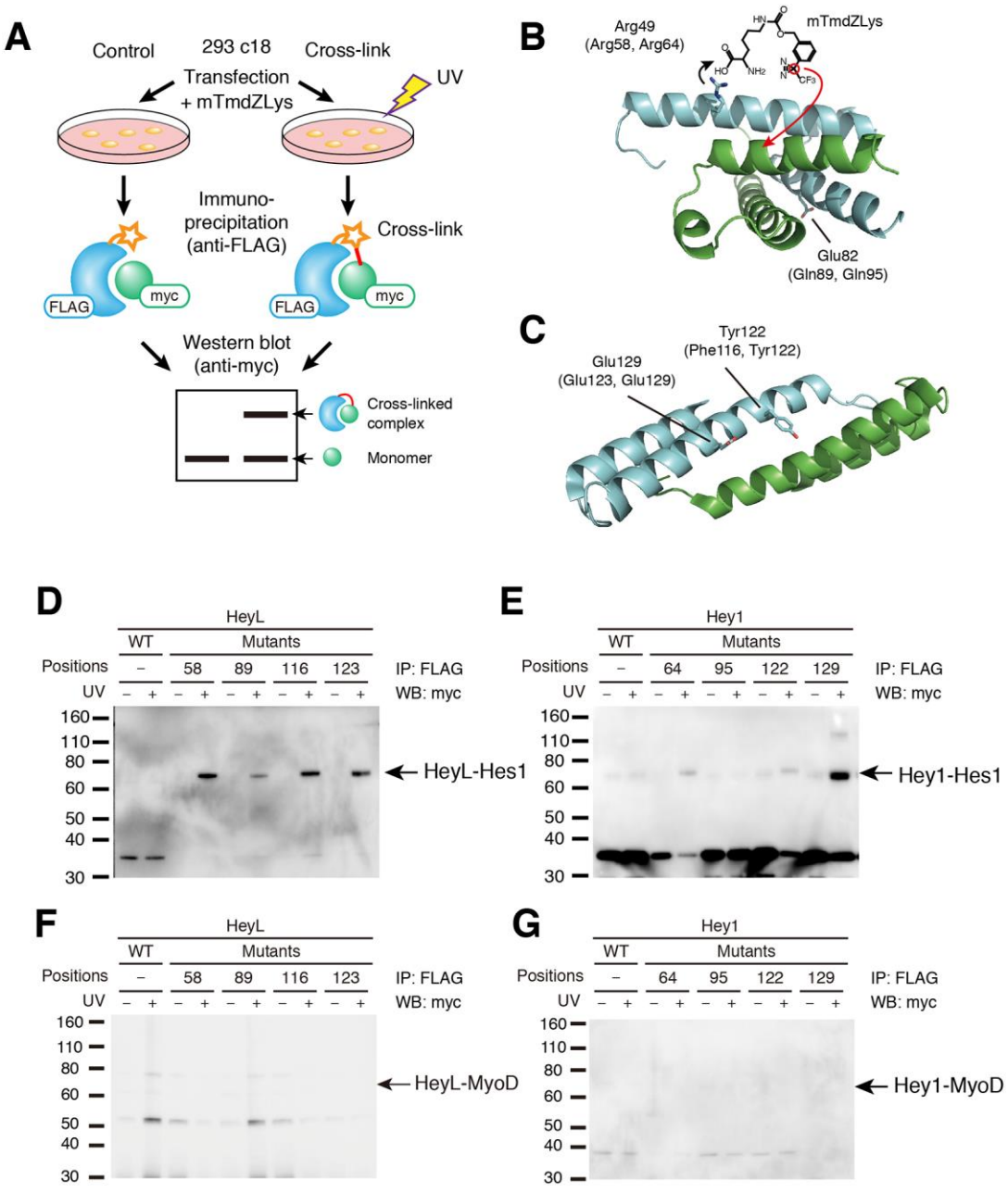

Figure 4: HeyL forms heterodimer complex with Hes1 in living cells

(A) Experimental procedure for the photo-cross-linking of heterodimers between Hey1, HeyL, Hes1, and MyoD, and the following analysis.

(B, C) Homodimer complex structures of the human HES1 Orange domain (B) and the human HEY1 bHLH domain (C) obtained from the Protein Data Bank (ID: 2MH3 and 2DB7, respectively). The residue positions chosen for the substitution with mTmdZLys are indicated. The homological residues of mouse HeyL (Orange domain; positions 58

and 89, bHLH domain; positions 116 and 123) and Hey1 (Orange domain; positions 64 and 95, bHLH domain; positions 122 and 129) are indicated in parentheses.

(D) Western blotting for analysis of the photo-cross-linking between HeyL-Hes1. Wild type HeyL (WT) and its mutants containing mTmdZLys at indicated positions, tagged with FLAG peptide, were co-expressed with myc-tagged Hes1 in 293 c18 cells. HeyL complexes were immunoprecipitated with an anti-FLAG antibody from extracts of the cells that were exposed or not to UV. Cross-linked complexes of HeyL and Hes1 were detected with an anti-myc antibody.

(E) Western blotting for the analysis of photo-cross-linking of Hey1-FLAG with Hes1-myc (E), HeyL-FLAG with MyoD-myc (F), or Hey1-FLAG with MyoD-myc (G).

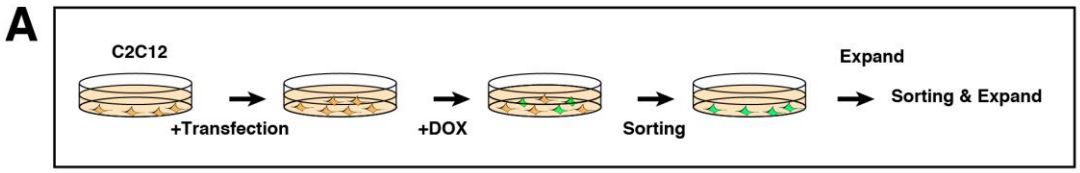

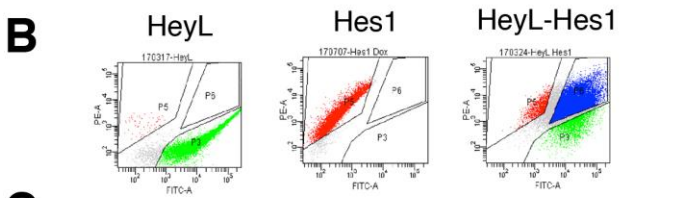

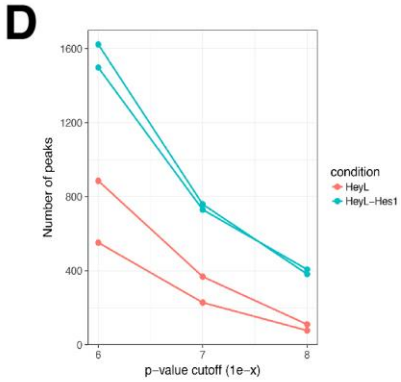

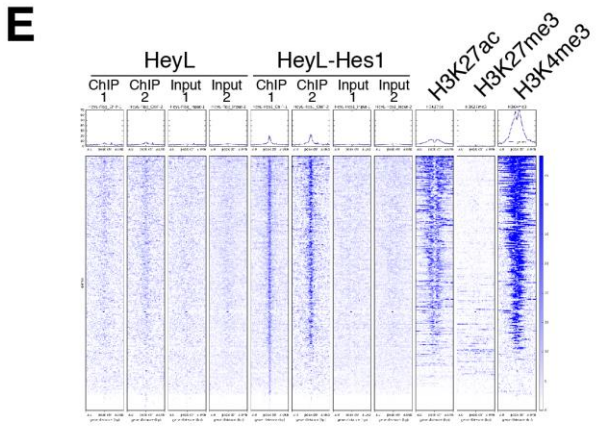

F

Rank	Motif	Name	E-value	% of targets
1		HEY1	6.3e-10	33.77%
2		Arnt	2.0e-07	40.05%
3		HEY2	6.0e-6	41.36%
4		Tcfl5	1.0e-5	41.88%
5		Ahr::Arnt	3.1e-05	43.46%
6		Hes1	1.2e-4	42.15%
7		NRF1	1.0e-3	32.98%
8		BHLHE40	1.4e-3	33.51%

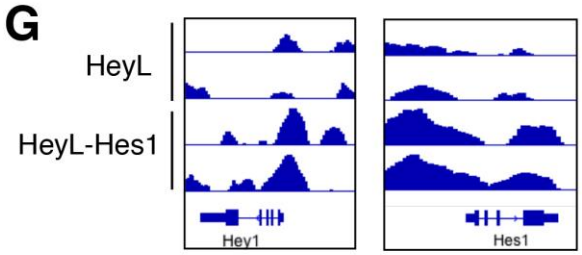

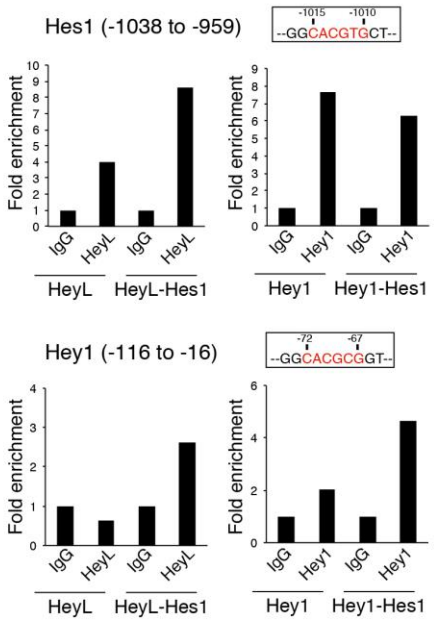

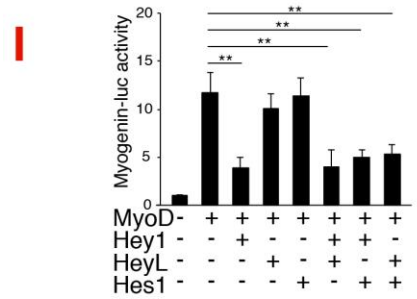

Figure 5: Co-existing HeyL and Hes1 bind to diverse DNA sites and synergistic effect

(A) Experimental procedure for the preparation of doxycycline (Dox)-dependent Hey1-, HeyL alone- or HeyL-Hes1-expressing C2C12 cells.

(B) FACS profile of Dox-treated HeyL-alone (EGFP) or HeyL-Hes1 (EGFP and mKO)-expressing C2C12. The results of Hes1 alone are also shown as the reference for mKO fluorescence.

(C) Signal distributions of HeyL and Hes1 normalized to the corresponding input data around the peak centers for the union of peaks for four samples (left) and around TSS's (right).

(D) The numbers of HeyL alone and HeyL-Hes1 peaks detected at various p-value cutoffs. The number is greater for HeyL-Hes1 for each case.

(E) Heat map for the signal of HeyL alone, HeyL-Hes1, H3K27ac, H3K27me3, and H3K4me3 within 3 kb around HeyL-Hes1 peak centers (replicate 1).

(F) Enriched motifs identified in regions bound preferentially by HeyL-Hes1.

(G) Integrative Genomics Viewer (IGV) images illustrating the signal for HeyL alone and HeyL-Hes1 normalized to the corresponding input signal at *Hey1* and *Hes1* gene loci. Here only positive log2 ratios are shown.

(H) Chip-PCR analyses were performed using HeyL alone, HeyL-Hes1, Hey1 alone or Hey1-Hes1 expressing C2C12 and control IgG and anti-FLAG antibodies. Immunoprecipitated DNA fragments were analyzed by real-time PCR with specific primers to Hes1 promoter regions (-1038 to -959 site) containing 'CACGTG' motif or Hey1 promoter regions (-72 to -67 site) containing 'CACGCG' motif. The numbers mean positions relative to the transcriptional initiation site (+1). Y-axis indicates the average from two to three independent experiments.

(I) Relative luciferase activities of MyoD or MyoD co-transfected with Hey1, HeyL, and/or Hes1 expression plasmids in C2C12. Y-axis indicates the average from three to five independent experiments with SD. **, $P<0.01$.

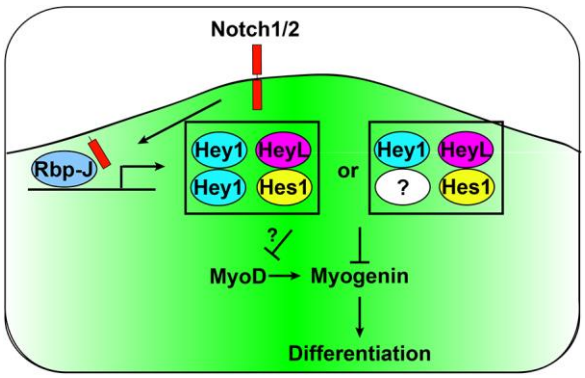

Figure 6: Hey1, HeyL, and Hes1 in muscle stem cells are required for maintaining the undifferentiated state.

HeyL-Hes1 and Hey1 homodimer/heterodimer are two essential units downstream of the canonical Notch pathway in MuSCs.

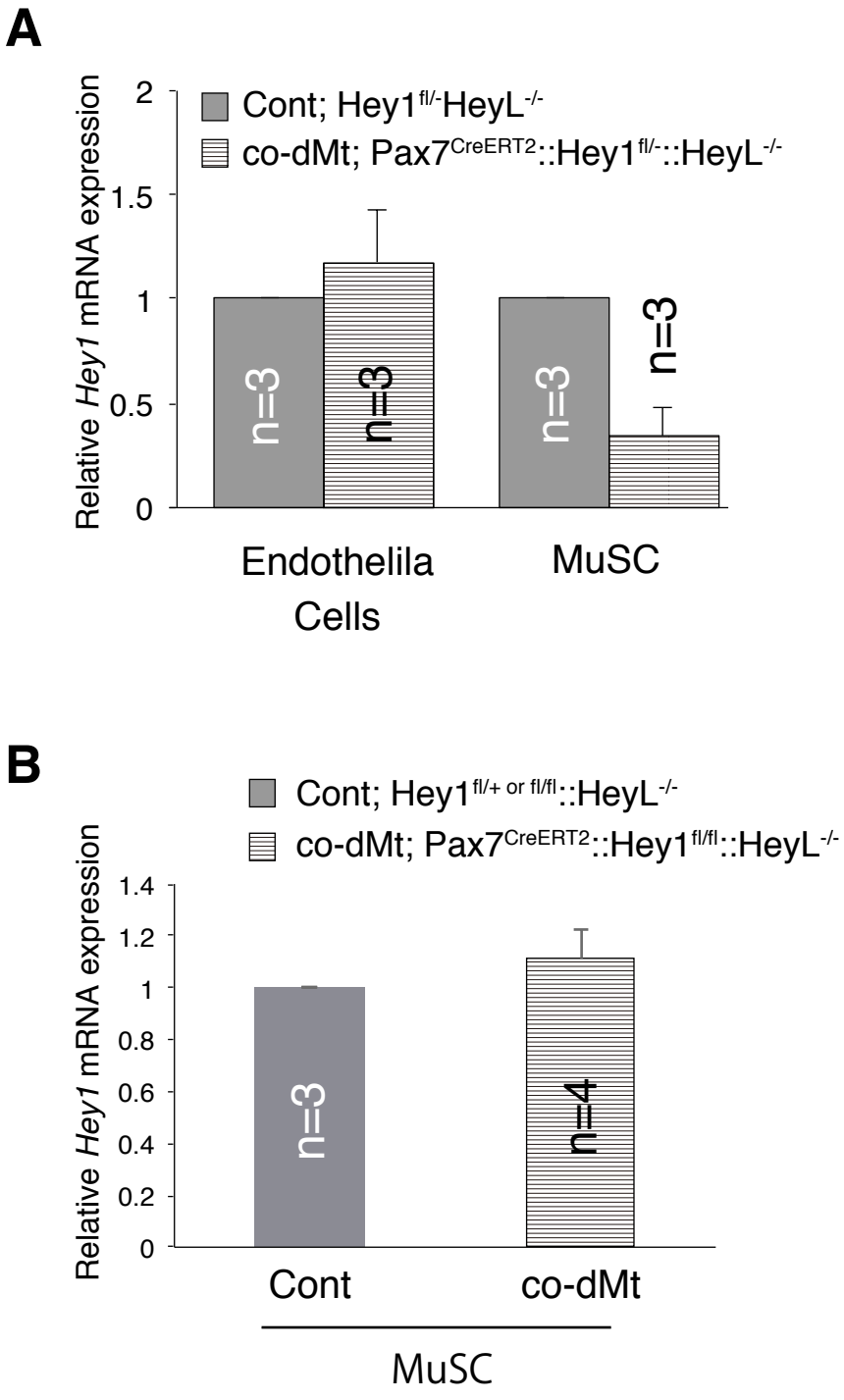

Figure S1. Hey1 mRNA levels of 4- or 9-week-old mice

A; Reduced Hey1 mRNA expression in muscle stem cells, but not in endothelial cells

Relative mRNA expression of *Hey1* gene in freshly isolated MuSCs and endothelial cells derived from Cont (Gray bar; $Hey1^{flox/-}$::$HeyL^{-/-}$) or co-dMt (Stripe bar; $Pax7^{CreERT2/+}$::$Hey1^{flox/- \text{ or } flox/flox}$::$HeyL^{-/-}$ without Tm) mice at 9 weeks old.

B: Hey1 mRNA expression is not changed in co-dMt untreated with tamoxifen at 4 weeks old.

Relative mRNA expression of the *Hey1* gene in freshly isolated MuSCs from Cont (Gray bar; $Hey1^{flox/-}$::$HeyL^{-/-}$) or co-dMt (Stripe bar; $Pax7^{CreERT2/+}$::$Hey1^{flox/- \text{ or } flox/flox}$::$HeyL^{-/-}$ without Tm) mice at 4 weeks old.

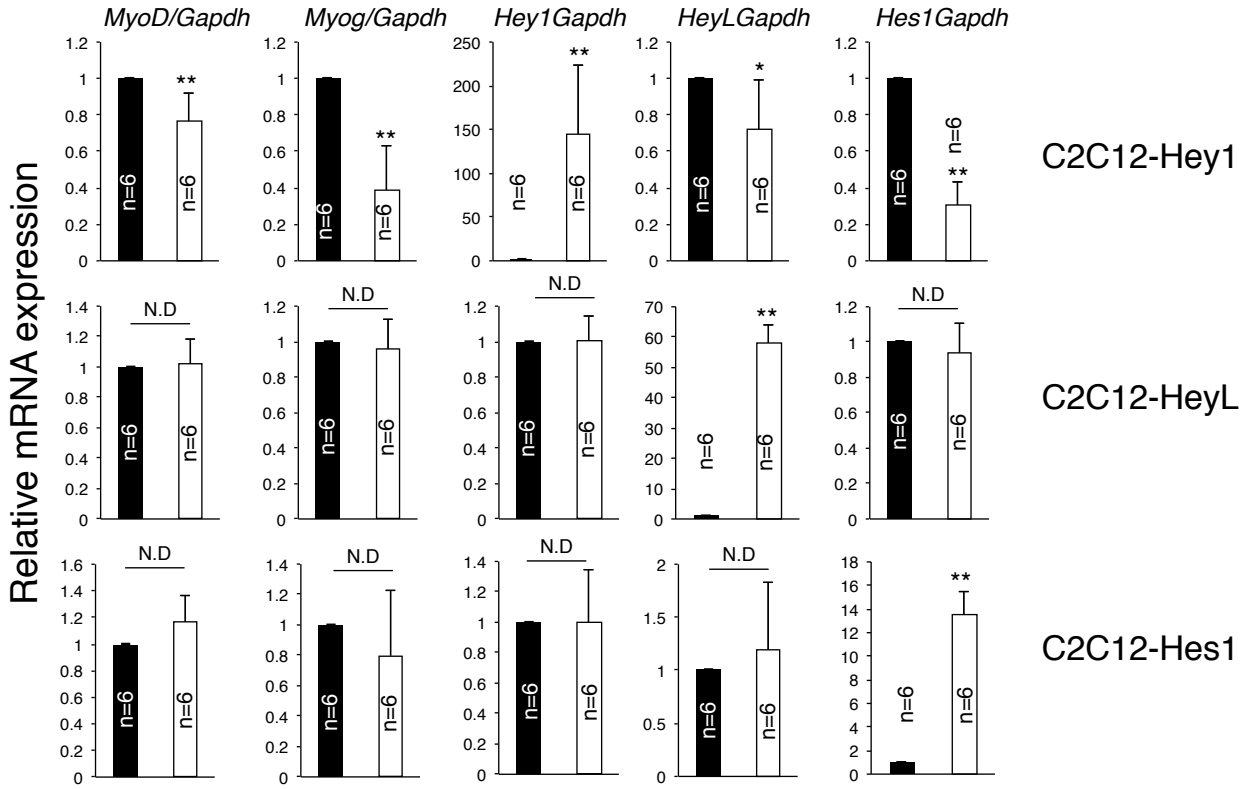

Figure S2. Hey1 has anti-myogenic effect, but not HeyL and Hes1

Relative mRNA expression of indicated genes in control (Black bar; Dox-) or Hey1, HeyL, or Hes1 expressing C2C12 (White bar; Dox+). *; P<0.05; **, P<0.01.

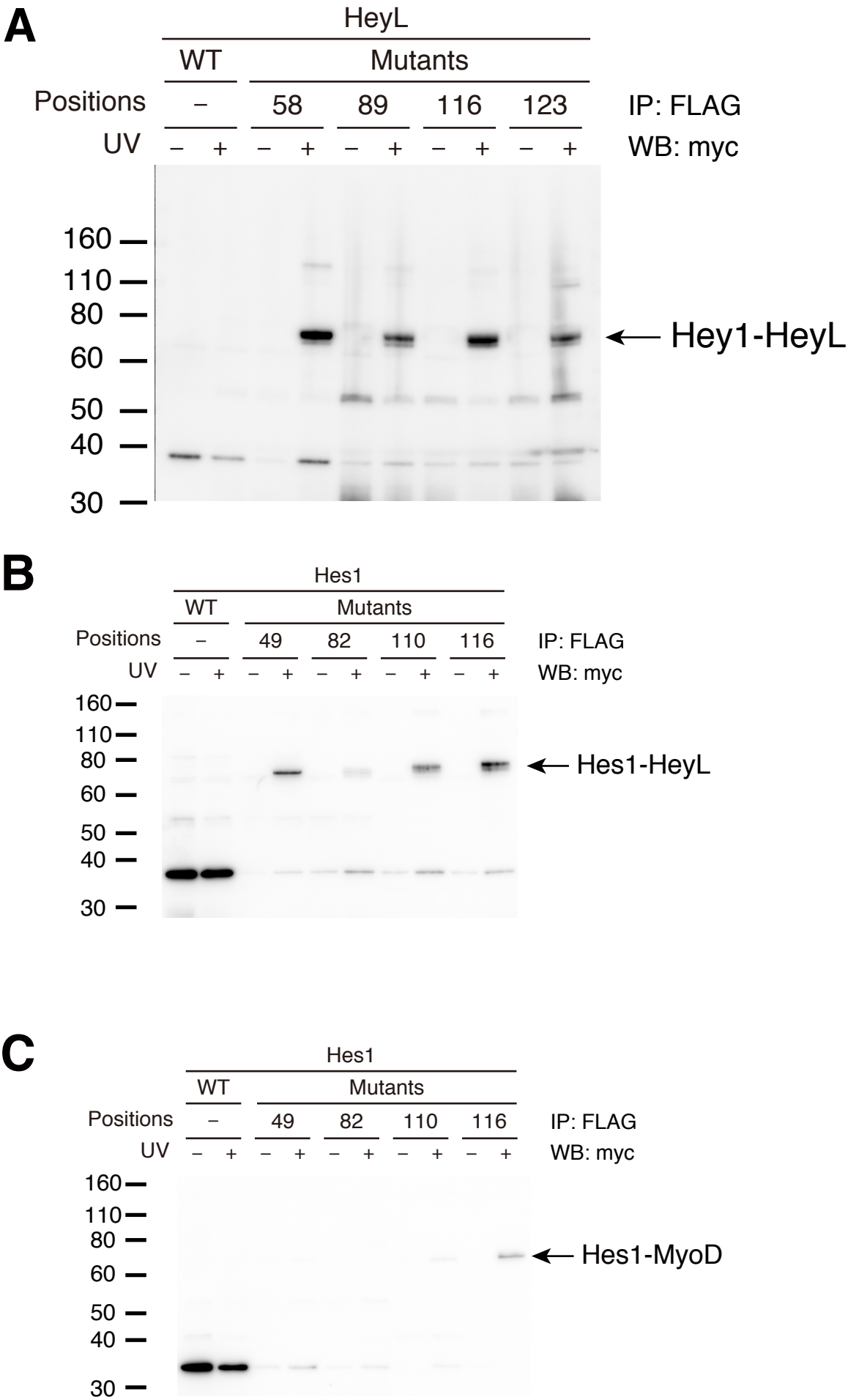

Figure S3. HeyL forms a heterodimer complex with Hey1 in living cells

A: Western blotting for analysis of photo-cross-linking of HeyL-FLAG with Hey1-myc. Site-specific incorporation of mTmdZLys into the Orange (positions 58 and 89) and bHLH (positions 116 and 123) domains of HeyL in 293 c18 cells, protein photo-cross-linking in the cells, and subsequent purification and detection of cross-linked products were performed as described in Figure 4.

B, C: Western blotting for analysis of photo-cross-linking of Hes1-FLAG with HeyL-myc (B), and of Hes1-FLAG with MyoD-myc (C). Site-specific incorporation of mTmdZLys into the Orange (positions 49 and 82) and bHLH (positions 110 and 116) domains of Hes1 in 293 c18 cells, protein photo-cross-linking in the cells, and subsequent purification and detection of cross-linked products were performed as described in Figure 4. While cross-linked complexes between Hes1 and HeyL were clearly detected at about 70 kDa (B), complexes between Hes1 and MyoD were only faintly detected (C). These results indicated that Hes1 interacted with MyoD much less efficiently than with HeyL in the 293 c18 cells.

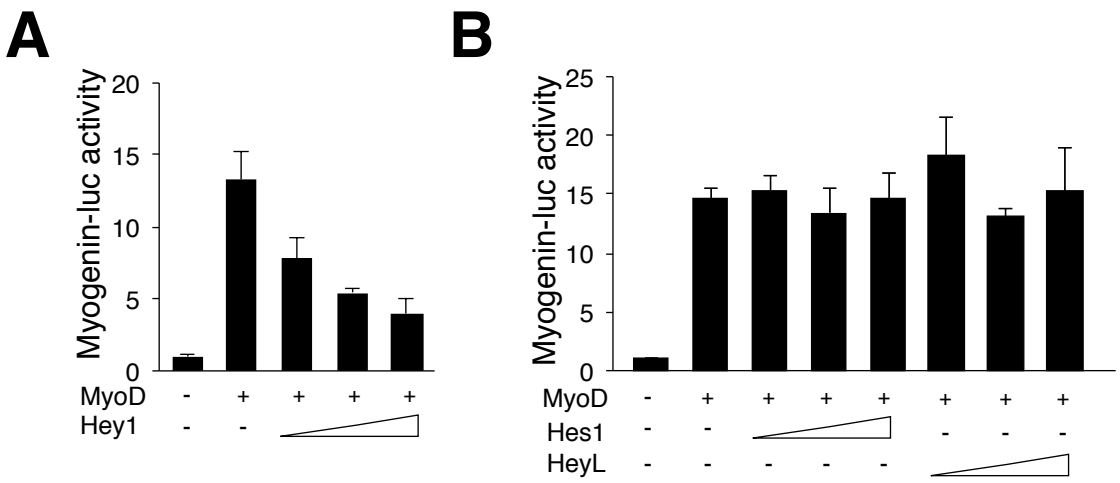

Figure S4. HeyL or Hes1 alone did not suppress MyoD-dependent myogenin promoter activity

A: Relative myogenin-luciferase activities in MyoD cells transfected or co-transfected cells with Hey1 expression plasmids in C2C12. The Y-axis indicates the average results from four independent experiments with SD. **, P<0.01.

B: Relative myogenin-luciferase activities in MyoD cells transfected or co-transfected with HeyL or Hes1 expression plasmids in C2C12. The Y-axis indicates the average results from four independent experiments with SD. **, P<0.01.

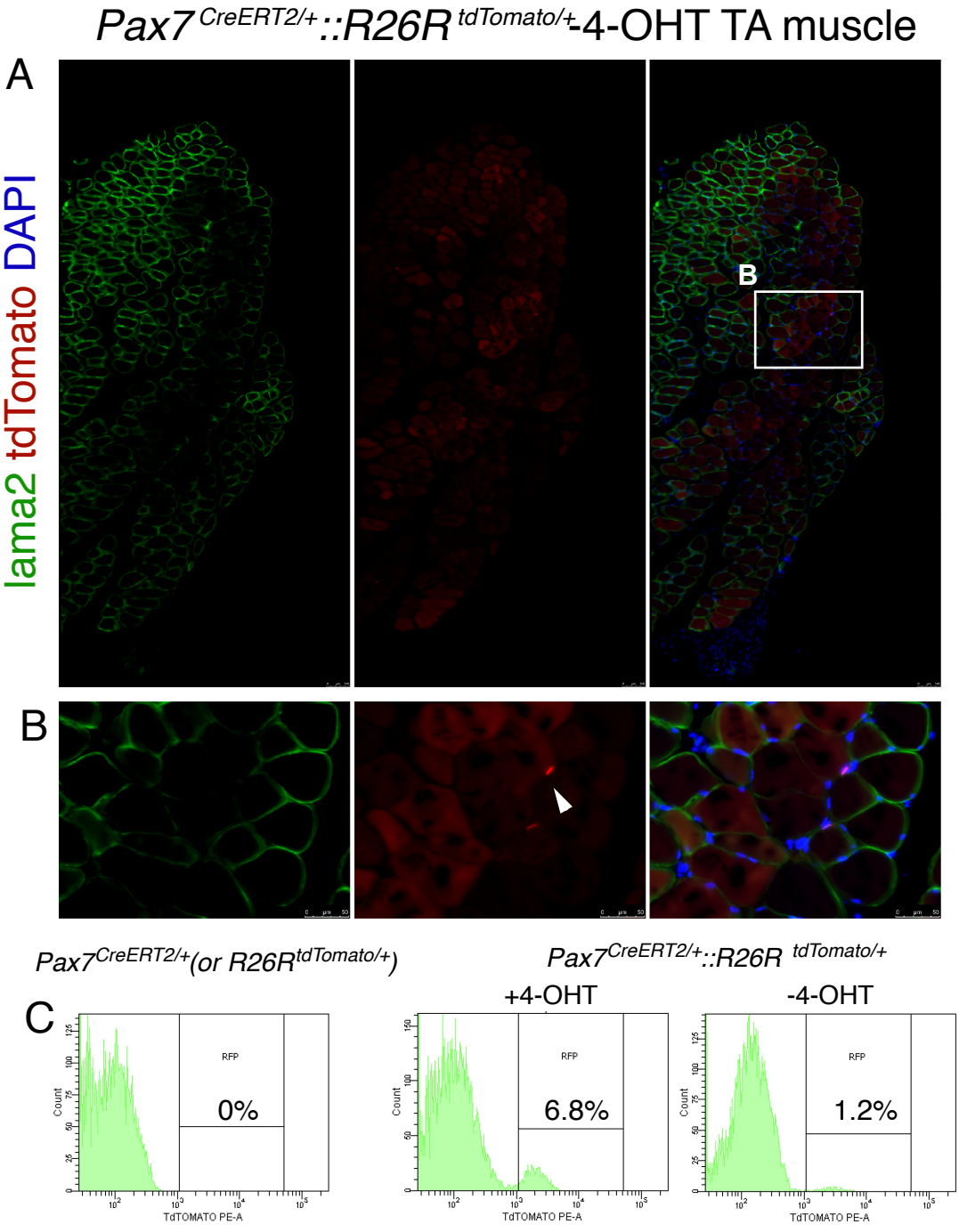

Figure S5. Tamoxifen-independent Cre recombination in *Pax7*$^{CreERT2/+}$ mice::*R26R*$^{tdtomato/+}$.

A, B: Uninjured tibialis anterior muscle (TA) of 4-hydroxy tamoxifen (4-OHT) untreated *Pax7*$^{CreERT2/+}$ mice::*R26R*$^{tdtomato/+}$ mice were stained with anti-laminin α2 (lama2; green) antibody and DAPI (blue). Arrowheads show muscle stem cells expressing tdTomoto (red) (B, magnified image of A) in 4-OHT untreated *Pax7*$^{CreERT2/+}$ mice::*R26R*$^{tdtomato/+}$ mice.

C: The frequency of tdTomato-positive muscle stem cells in control (*Pax7*$^{CreERT2/+}$ or *R26R*$^{tdtomato/+}$ mice), 4-OHT-treated (+4-OHT), or untreated (-4-OHT) *Pax7*$^{CreERT2/+}$ mice::*R26R*$^{tdtomato/+}$ mice.